Cell Regeneration 8 (2019) 58–71

Contents lists available at ScienceDirect

Cell Regeneration

journal homepage: http://www.keaipublishing.com/en/journals/cell-regeneration/

Original Article Type

Bone marrow-derived mesenchymal stem cell (BM-MSC): A tool of cell therapy in hydatid experimentally infected rats

Faten A.M. Abo-Aziza [a, *], Abdel Kader A. Zaki [b], Amal M. Abo El-Maaty [c]

[a] Department of Parasitology and Animal Diseases, Veterinary Research Division, National Research Centre, Cairo, Egypt
[b] Department of Veterinary Medicine, College of Agriculture and Veterinary Medicine, Qassim University, Buraydah, Saudi Arabia
[c] Department of Animal Reproduction and AI, Veterinary Research Division, National Research Centre, Cairo, Egypt

ARTICLE INFO

Article history:
Received 12 September 2019
Received in revised form
30 October 2019
Accepted 1 November 2019
Available online 21 November 2019

Keywords:
Bone marrow
Mesenchymal stem cell
Cell therapy
Hydatid

ABSTRACT

This study aimed to clarify the potentiality of bone marrow mesenchymal stem cells (BM-MSC) transplantation with albendazole (ABZ) on the modulation of immune responses against hydatid cyst antigens and the regeneration of injured livers in experimentally infected rats. Three different antigens of hydatid cyst fluid (HCF), hydatid cyst protoscolex (HCP) and hydatid cyst germinal layer (HCG) were isolated and their antigenic potencies were determined. The ultrasound, immunological and pathological criteria were investigated. Counting of 80% confluence BM-MSC was 4.68×10^4 cells/cm^2 with 92.24% viability. Final population doublings score was 65.31 that indicated proliferation and self-renewability. Phenotyping of BM-MSC showed expression of CD73 and CD29 without exhibition of CD34 and CD14. Ultrasound examination showed multiple hydatid cysts in liver with low blood flow and spleenomegaly 8 weeks' post infection. No significant differences were noted in cystic diameter in uni-cyst liver at 2nd and 4th weeks following ABZ treatment while it was significantly decreased ($P < 0.05$) following transplantation of BM-MSC + ABZ treatment comparing to experimentally infected untreated group. Igs and IgG responses to the three antigens were significantly elevated while elevation in IgM response was only to HCG ($P < 0.05$). ABZ treatment accompanied with significant decrease in Igs and IgG titers against HCF and HCG only at 4th week post treatment ($P < 0.05$). However, Igs titer against HCF, HCP and HCG was significantly decreased at the 4th week following transplantation of BM-MSC + ABZ. Interestingly, the combination of BM-MSC + ABZ treatment resulted in reduction of Igs response to HCP to normal level as that of healthy control. Experimental infection resulted in elevation of TNF-α and IL-6 ($P < 0.05$) while, IL-4 and IL-10 decreased ($P < 0.01$). After transplantation of BM-MSC + ABZ treatment, serum TNF-α and IL-6 concentrations were reduced ($P < 0.05$) at both the 2nd and 4th weeks. However, IL-4 and IL-10 concentrations were significantly elevated ($P < 0.05$) only at 4th week following transplantation of BM-MSC + ABZ treatment. In conclusion, BM-MSC transplantation following ABZ administration can regenerate injured liver tissue without complete disappearance of hydatid cyst. In addition, it can modulate host protective humeral and cell mediated immune responses against hydatid cyst antigens. Therefore, the current study encourages to move to the step of performing clinical trials in humans.
© 2019 Chinese Society for Cell Biology (CSCB). Production and hosting by Elsevier B.V. on behalf of KeAi. This is an open access article under the CC BY-NC-ND license (http://creativecommons.org/licenses/by-nc-nd/4.0/).

1. Introduction

Hydatidosis is a worldwide zoonotic disease caused by *Echinococcus* which is a genera of tapeworm parasites that is important in the Mediterranean region [1]. Cystic hydatidosis in the intermediate hosts is a complex disease that becomes major public health problem in many countries despite being, in principle, preventable, treatable, and eradicable [2]. Effective treatments as well as well-designed immunomodulation are poor and the trials that could guide therapy are overdue [3].

The effectiveness of parasite control programs is limited due to the severe deficiency of immunity to reinfection in the definitive host and the high accessibility of infected intermediate hosts [4]. In addition, the *Echinococcus* organisms, can modulate the immune

* Corresponding author. Department of Parasitology and Animal Diseases, Veterinary Research Division, National Research Centre, 33 El-Bohouth street, Dokki, Cairo, 126222, Egypt.
E-mail address: faten.aboaziza@gmail.com (F.A.M. Abo-Aziza).
Peer review under responsibility of Chinese Society for Cell Biology (CSCB).

https://doi.org/10.1016/j.cr.2019.11.001
2045-9769/© 2019 Chinese Society for Cell Biology (CSCB). Production and hosting by Elsevier B.V. on behalf of KeAi. This is an open access article under the CC BY-NC-ND license (http://creativecommons.org/licenses/by-nc-nd/4.0/).

responses to persist and flourish in their hosts [5]. The parasite protects its own survival, by using both defensive and down-regulatory mechanisms. During infection, the outer tegumental coat and the continuously release excretory/secretory products are considered the two major sources of modulatory antigens. Both of these antigens are constantly interact with cells of the host's immune system to provoke immune-modulatory episodes. Moreover, the cyst plays a major role as a protective shelter from both destruction and detection. This down-regulation of the immune system produces a downhill, where the lack of stimuli also reduces the response [5]. Anthelmintics is the main choice in the control measures for these cysts forming parasites. Chemotherapy with albendazole (ABZ) still used for hydatid disease control, due to its broad spectrum and safety [6]. Usually, treatment with drugs not give 100% curing results even if the drug targets either the parasite or the liver, therefore, additional tools are needed for hydatid disease control [7].

Liver is the most commonly affected organ with hydatid cyst due to the priority of its capillary fields that encountered by the blood borne oncospheres of the parasite [1]. The larval mass usually results in irreversible fibrosis [8]. The liver hid high number of small sized and calcified cysts which occurred due to a high reticuloendothelial cells and abundant connective tissue reaction [9]. Despite of the considerable intrinsic regenerative capability of the liver, persistent and chronic damage may lead to liver fibrosis [10]. It is not improbable that larger number of embryos is killed in these organs, the site of destruction and lesion usually cured by fibrosis and calcification [1].

The cyst or even the affected segments of the liver resection are often performed surgically. The success rate varies with the *Echinococcus* species and the location and size of the cysts and in some cases, it may be not possible to remove the entire cyst [11]. In addition, long-term post-surgical treatment with anthelminthic drugs are required. Another choice of management of hydatid cyst is PAIR (puncture, aspiration, injection, and re-aspiration) technique [12]. The PAIR technique is one of the non-invasive approach in which the aspiration of cyst contents and injection of an anthelminthic drug instead was done under ultrasonographic direction. However, the multiple hydatid cyst is very invasive and also metastasizes, therefore, a complete surgical curing is rare except in the early stages of infection [11]. In the last few years, surgical interference for liver transplantation for end-stage liver fibrosis was an option [13]. However, high risk of liver transplant immunological rejection, shortage of donor organs, surgical complications and high medical costs restrict the usage of the most appropriate option for severe acute and chronic liver diseases [14]. Hepatocyte transplantation, has hardly produced the required therapeutic effects due to unresolved problems of functional hepatocytes *in vitro* maintenance and amplification [15]. Therefore, the developing of an alternative source of cells that can be isolated and differentiated into functional hepatocytes is required urgently [16]. There are many cell sources but it is not clear which will verify the therapeutic optimality [17]. Mesenchymal stem cells (MSC) are the best hope for effective different cell types [10]. Several studies have indicated that MSC were effective in the regeneration of injured tissues, reduction of inflammatory oxidative stress and immune modulation [18]. More attention has recently directed to bone marrow mesenchymal stem cells (BM-MSC) for their therapeutic potential in regenerative medicine [19]. Recently, BM-MSC transplantation has been suggested as an effective alternative therapy for hepatic regeneration because of their hepatogenic differentiation potential as well as their immune–modulatory properties and their trophic factors secretion capacity [20]. In this study, it is hypothesized that, the combined BM-MSC transplantation and ABZ treatment can overcome the poor results of ABZ alone or the complications of other techniques. Beside the effect of ABZ therapy, BM-MSC is transplanted to modulate the immune responses against antigen and regenerate injured tissues. To approve this hypothesis, experimental infection of hydatid cyst protoscolices in rats was done. The therapeutic potential of combining BM-MSC transplantation with ABZ in hydatid experimentally infected rats was investigated comparing with using ABZ alone. Liver regeneration of experimentally infected rats was investigated by ultrasound, and histopathological examination. Immunomodulation was monitored by measurement of immunoglobulins, leukocytes, splenocytes viability, phagocytosis index, Th1 (TNF-α, IL-6) and Th2 (IL-4, IL-10) cytokines.

2. Materials and methods

2.1. Ethics statement

All animal experiments were approved by Institutional Animal Care and Use Committee of National Research Centre (Protocol Number: 16/230), Cairo, Egypt.

2.2. Preparation of hydatid cyst antigens

Three hydatid cyst antigens were prepared [21]. Hydatid cysts were collected from infected livers and lungs of the slaughtered camels. Hydatid cyst fluid was aseptically aspirated (Fig. 1-A) and centrifuged at 13000 rpm for 20 min in cooling centrifuge. The supernatants were collected, dialyzed and stored as hydatid cyst fluid (HCF) antigen at −20 °C. Protoscolices were obtained from sediment of collected cyst fluid. They were washed twice and resuspended with phosphate-buffered saline (PBS, pH 7.2). The protoscolices were exposed to 3 cycles of freezing, thawing and sonication (1 min, 0.5 amplitude), then they were microscopically checked until no intact protoscolices were detected. The protoscolex antigens were centrifuged at 10000 rpm for 30 min in a cooling centrifuge. The supernatants were collected and stored as hydatid cyst protoscolex (HCP) antigen at −20 °C. Germinal layers of hydatid cysts were dissected (Fig. 1-B), washed several times and homogenized in PBS pH 7.2. The homogenate was sonicated for 3 cycles (1 min, 0.5 amplitude) and centrifuged at 10000 rpm for 30 min. The supernatants were aspirated and stored as hydatid cyst germinal layer (HCG) antigen at −20 °C.

2.3. Determination of total protein contents of different prepared antigens

Total protein contents of HCF, HCP and HCG antigens were measured according to Bradford assay [22]. The assay depended on home-made Bradford reagent; 0.01% Coomassie brilliant blue G-250 (Jena Bioscience, USA), 5 ml absolute ethanol and 10 ml 85% phosphoric acid (Sigma–Aldrich, USA). Bovine serum albumin was used as standard. Optical densities (ODs) were measured

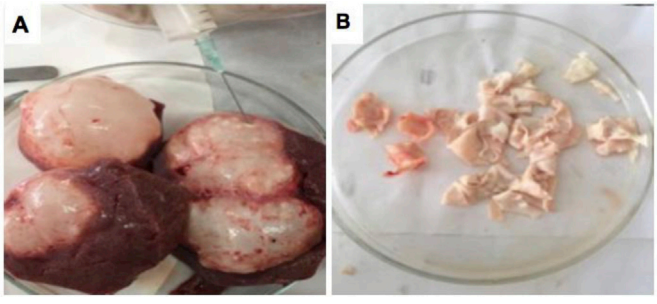

Fig. 1. Hydatid cyst of camel showing aspiration of the fluid from the cyst (A). Inner thin germinal layer collected from hydatid cyst (B).

spectrophotometrically at 595 nm. The total protein content was calculated by the following formula: Total protein content (mg/ml) = sample OD/standard OD x standard concentration. By determination of total protein contents in the prepared hydatid antigens, it was found that the HCF, HCP and HCG recorded protein content 0.403, 1.417 and 3.208 mg/ml respectively.

2.4. Preparation and determination of potency of antibodies against isolated antigens using indirect enzyme linked immunosorbent assay (ELISA)

Nine healthy native males' rabbits weighing 2–2.5 kg were used for preparation of antibodies against HCF, HCP and HCG antigens (3 rabbits for each antigen) [23]. Blood samples were collected from each rabbit to separate the control negative serum and kept at −20 °C. Each antigen was mixed with an equal volume of Complete Freund's Adjuvant (Difco, Detroit, MI, USA) and 1 mg/kg was subcutaneously injected at different sites weekly for four successive weeks. One week later, a booster dose of each antigen emulsified with Incomplete Freund's Adjuvant (Difco, Detroit, MI, USA) were injected subcutaneously. After one week, rabbit sera were tested by agar gel diffusion test to estimate the immunoglobulins value [24]. The rabbits were slaughtered, when the results were strongly positive. Sera were individually collected and stored at −20 °C until use.

Indirect ELISA were performed in order to evaluate the potency of the prepared IgG against HCF, HCP and HCG antigens [21]. Briefly, checker-board titration was done to optimize the concentration of different antigens, sera and conjugate. Wells were coated with different diluted antigens in carbonate buffer (PH 9.6) and incubated overnight at 4 °C. The wells were blocked with 1% bovine serum albumin, pH 9.6 for 1 h at room temperature, followed by the addition of diluted sera (1:50) in 0.05% PBS-T-20 and incubated for 2 h. After washing, 100μl/well of protein-A peroxidase conjugate were added and incubated for 1 h at 37 °C followed by addition of substrate solution (O, phenylenediamine, one tablet 20 mg/ml). ODs were read at wave length of 450 nm with an ELISA reader (MR 700 Microplate Reader A Dynamic product, USA). The results obtained from the log-dose response curves of the standard HCF, HCG and HCP antigens revealed that the slope of regression (b) among the graded log-doses and their corresponding ODs were 0.322, 0.344 and 0.326 respectively.

2.5. Experimental infection of rats with hydatid cyst protoscolices

Hydatid cyst fluid was aseptically aspirated from freshly collected hydatid cysts for experimental infection in rats [25]. The aspirated fluid was left to settle the protoscolices for 30 min. The sedimented protoscolices were collected and washed with normal saline. The viability of the protoscolices was confirmed by flame cell activity and general contractile motility under an optical microscope. The protoscolices were diluted and adjusted to concentration of 1000/100 μl. Eighteen rats were obtained and reared at animal house of National Research Centre. All rats were kept under good condition and offered a balanced ration. The rats were injected with 1000 protoscolices of fresh camel hydatid cyst in normal saline for 8 Wks. The implantation of hydatid cyst protoscolices and growing dynamics of the infection were estimated by ultrasound.

2.6. Isolation of rat BM-MSC

BM-MSC was originally isolated and expanded from femurs bone of healthy albino rats [26]. The obtained cells were cultured at 15×10^6 cell density into 100 mm culture plate (Corning, USA) and incubated in 5% CO2 at 37 °C in alpha minimum essential medium (α-MEM, Sigma-Aldrich, USA) containing 20% fetal bovine serum (FBS), L-glutamine (2 mM), 2-mercaptoethanol (55 μM) and penicillin/streptomycin. After reaching 80% confluence in the 3rd passage BM-MSC were collected and exposed for their characterization and proliferation assays.

2.7. Characterization of BM-MSC by cell counting, viability and phenotyping analysis

At the 3rd passage of rat BM-MSC, the cells were detached, collected and centrifuged at 2000 rpm for 5 min. The cells were then suspended in 2 ml α-MEM and their number was counted in an aliquot using hemocytometer. The viability of BM-MSC was evaluated and the dead cells were excluded using trypan blue stain [27]. For BM-MSC surface antigen phenotyping, cell markers were analyzed as described previously [15]. Briefly, 0.2×10^6 cells were washed two times with PBS containing 1% bovine serum albumin (Sigma–Aldrich, USA). The cells were then stained with anti-CD34, anti-CD14, anti-CD73, and anti-CD90 antibodies (BD Biosciences). Conjugated cells were examined by a FACS Calibur flow cytometer (BD Biosciences) and isotype was used as control.

2.8. Cell proliferation assay

To determine the proliferation capacity of BM-MSC, CFU-F assay and population doubling (PD) assay were performed. For CFU-F assay, one million cells from the 3rd passage of BM-MSC were seeded on 100 mm culture dish. Upon reaching 80% confluence the cultured cells were washed and the cells were examined under inverted microscope. Each cell group containing in excess of 50 cells was counted as colony [28]. PD assay was calculated [29] A total of 0.25×10^6 cells was seeded on culture flasks and upon reaching 80% confluence, the cells was detached using Trypsin–EDTA and then passaged. The cells were monitored and the number was counted at every passage. PD in each passage was estimated as follow: $\log_2$ (number of collected cells/number of cultured cells). The final PD was calculated by accumulation of the total numbers of each passage until the cell division cease.

2.9. ABZ treatment and BM-MSC transplantation

2.9.1. BM-MSC transplantation

Transplantation of BM-MSC into hydatid-infected rats was done at 8th Wk post infection by single intrahepatic injection using 1.5×10^6 cells/rat suspended in low glucose Dulbecco's Modified Eagle Medium (DMEM; Sigma–Aldrich, USA) with L-glutamine (2 mM), and 20% FBS. Rats abdomen were shaved and the skin was sterilized with alcoholic solution [30]. The liver site was defined to be the area of injection in each rat. The dose was directly injected in this area very slowly over a 10-min to prevent the obstruction of the needle.

2.9.2. ABZ treatment

A suspension of ABZ (EIPICo. Pharmaceuticals) was supplemented orally at a dose of 15 mg/kg/day at 8th Wk post infection for 14 days in divided doses twice daily [6].

2.9.3. Experimental design

Twenty-four male albino rats were used. Six rats were injected with DMEM and considered as healthy control group. The eighteen hydatid infected rats were divided into 3 subgroups (n = 6/subgroup). The first subgroup was injected with DMEM and considered as infected non-treated group. The 2nd subgroup was treated with ABZ. The 3rd subgroup was transplanted with BM-MSC following ABZ. Blood samples were

collected at 2nd Wk post transplantation (PT) followed by scarification of all rats at the 4th Wk PT. Half of the blood was taken into EDTA containing tubes for hematological study. The other half was collected in plain tubes and sera were separated by centrifugation of blood at 3000 rpm/15min to be suspected for immunological and cytokines analysis. Livers and spleen were gently removed for histopathological examination. Spleen specimens were used for preparation of splenocytes.

2.10. Ultrasound examination

The rats were examined by ultrasound at the 2nd and 4th Wks PT [31]. The rats were shaved and anesthetized with xylazine 10 mg/kg immediately before examination. All rats were screened by using a pulsed-wave Doppler ultrasound scanner mode (B, color, spectral and power Doppler) equipped with 12 MHz linear-array transducer for liver and spleen examination. Cyst lesions including location, shape, boundary, diameter, echogenicity and features were recorded. The hepatic and splenic blood flow and direction were quantified from the color images using color and power flow mode. Regions with a flow velocity higher than 10 mm/s were represented by colored areas. All scans were done at 6 Hz pulse-repetition frequency. When a cardiac cycle was observed in the hepatic artery, the spectral mode was activated and the blood flow was traced by measuring the peak systolic velocity (PCV), end diastolic velocity (EDV), systolic/diastolic (S/D), time average maximum velocity (TAMV), pulsatility index (PI) and resistance index (RI).

2.11. Histopathological examination

Livers tissue specimens were collected from rats at the end of the experiment and immediately fixed in 10% neutral buffered formalin. The fixed specimens were undergone in the ordinary processing before embedding in paraffin wax. Thin sections were performed and stained with hematoxylin and eosin (H&E) [25].

2.12. Humeral immune response

2.12.1. Determination of total immunoglobulins by solid phase ELISA

Solid phase ELISA was performed for detection of different immunoglobulins in sera of the different groups of rats [32]. Briefly, each prepared antigen (HCF, HCP and HCG) was diluted to desired concentration in PBS. Each antigen (100 µl/well) was added to be attached directly to the bottom of the ELISA plate wells. The plates were incubated overnight at 4 °C. Each plate was blocked with 1% skim milk in PBS at 37 °C for 2 h. Serial dilution of serum samples (100 µl/well) were added to the plates at 37 °C for 2 h then incubated overnight at 4 °C. Enzyme conjugate horseradish peroxidase labeled goat anti-mouse immunoglobulin (Sigma-Aldrich, USA) at a titer obtained from checker-board titration (1:2000). The plates were incubated for 1 h at 37 °C. Enzyme substrate solution containing Orthophenylenediamine (OPD, Sigma–Aldrich, USA) was added to all wells. The plates were incubated in the dark for 7 min at room temperature. Peroxidase substrate was added; 100 ul to each well. The plates were covered and incubated for approximately 45 min at room temperature. The reaction was stopped with 50µl/well of H2SO4 2.5 M. The color reaction was measured at wavelength 450 nm using microplate ELISA reader (MR 700 Microplate Reader A Dynamic product, USA). The obtained ODs were considered as total immunoglobulins (Igs) anti-HCF, HCP and HCG antibodies. Fifty µl of 0.01 M mercaptoethanol in PBS was used instead of PBS alone, followed by the aforementioned procedure to obtain mercaptoethanol-resistant (IgG) level [33]. The differences between ODs of Igs and ODs of IgG were calculated as IgM antibody levels (mercaptoethanol-sensitive). The slope of regression “b" of the log dose response titer curves was obtained from respective standard preparation.

2.13. Cell mediated immune response

2.13.1. Eosinophil (EOS), neutrophil (N), lymphocyte (L) and N/L ratio

Counting EOS, N, L and N/L ratio were done by cross sectional method [34] Two blood films from each blood sample were prepared immediately after collection for staining. The blood films were fixed with methyl alcohol for 1–5 min and drown the alcohol off and allow to dry. Diluted Giemsa stain (20–30 drops) was added to the dried films and leave for 15–30 min before washing with distilled water and allowed to be dried. The stained blood films were then examined by using the oil emersion lens. A total of 100 leucocytes were counted using the straight edge method in which the cells were counted from one edge of the slide to the opposite edge and EOS, N, L and their ratio were calculated in percent.

2.13.2. Splenocytes viability

Splenocytes isolation was performed [35]. The spleen specimens were suspended in ice–cold RPMI-1640 medium (Sigma-Aldrich, USA) containing FBS (5%), 2 mM glutamine and two types of antibiotic. The specimens were then meshed with tweezers to release the splenocytes. The released cells were washed 2 times in RPMI-1640. Erythrocytes were lysed with warm isotonic ammonium chloride lysing solution. After centrifugation, the cells were resuspended in culture medium. Viability of splenocytes was evaluated by determining the viable cells number using trypan blue dye exclusion method.

2.13.3. Phagocytosis

In vitro carbon clearance assay was performed to determine the phagocytic index of T cells in blood [35]. Collected blood samples from each rat (1.5 ml) were mixed with 5 µl Indian ink. Each mixed sample was divided into 3 equal parts. Each part was diluted with 2 ml saline and incubated for 20 and 40 min at 37 °C, followed by centrifugation at 50 g for 4 min. The OD of supernatants were visualised by spectrophotometer at 535 nm, with a serum ink free sample as a blank. Phagocytic indices were calculated by converting the ODs to log [2] scale per hour.

2.13.4. Th1/Th2 cytokines measurement

Measurement of serum cytokines levels using ELISA was performed. Th1 cytokines; TNF-α and IL-6 and Th2 cytokines; IL4 and IL-10 concentrations were determined using ELISA kits (Sigma–Aldrich, USA). The manufacturer's instructions were followed and the color change was measured spectrophotometrically at a wavelength of 450 nm.

2.14. Statistical analysis

Descriptive values of data were represented as means ± standard errors. For statistical analysis, program SPSS version 19 and descriptive statistics and simple one way analysis of variance (ANOVA) was used with $P < 0.05$ and $P < 0.01$ being significantly different [36]. Duncan's Multiple Range test was used to detect statistical significant means at $P < 0.05$.

3. Results

3.1. Isolation, proliferation and characterization of BM-MSC

BM-MSC confluence was observed by inverted microscope after two days from initial seeding. Cells continued to proliferate and propagate to reach 50% and 80% confluence after one to two Wks respectively (Fig. 2). Cell counting, viability%, CFU-F and PD of BM-MSC upon reaching 80% confluence is shown in Table (1). The cell counting was 4.68×10^4 cells/cm^2 with 92.24% viability. *In vitro* study indicated that culture-expanded BM-MSC could produce extracellular matrix (ECM) and form CFU-F at a high extent. Final PD score was 65.31 that indicated attachment, proliferation, and self-renewal capacity of BM-MSC. By flow cytometric analysis, BM-MSC expressed MSC markers (Fig. 3). Particularly, BM-MSC showed negative expression of CD34 (0.56%), and CD14 (0.52%). However, BM-MSC positively expressed CD73 and CD29 (7.47% and 15.09% respectively).

3.2. Ultrasound examination

3.2.1. Ultrasonography images

In ultrasonography images, multiple hydatid cysts with a picture of low blood flow were shown in liver of hydatid experimentally infected untreated rats. Spleenomegaly with a picture of high blood flow was also shown in hydatid experimentally infected untreated rats. A stable single or multiple hydatid cysts were recorded in the liver besides spleenomegaly with low blood flow in liver and high blood flow in spleen at 2nd and 4th Wks following ABZ. Multiple and single small cysts were noted in liver following transplantation of BM-MSC + ABZ treatment at 2nd and 4th Wks respectively with normal spleen and normal picture of blood flow in liver and spleen (Fig. 4).

3.2.2. Morphometric ultrasonography analysis

Average spleen length and width diameter in hydatid experimentally infected untreated rats were significantly higher ($P < 0.05$) than healthy control rats. However, spleen length and width diameter decreased significantly ($P < 0.05$) at 2nd and 4th Wks following transplantation of BM-MSC + ABZ treatment comparing to untreated group. Moreover, average cystic diameters in uni-cyst and multi-cyst liver of untreated rats were 5.882 and 6.621 mm respectively. No significant differences were noted in cystic diameter in uni-cyst liver at 2nd and 4th Wks following ABZ treatment while it was significantly decreased ($P < 0.05$) following transplantation of BM-MSC + ABZ treatment comparing to untreated group (Table 2).

3.2.3. Blood flow of liver ultrasonography analysis

A picture of low blood flow of liver was observed in infected rats by means of significant low PSV, high EDV, low V mean ($P < 0.05$), high S/D, high G mean ($P < 0.01$) and high RI and PI ($P < 0.05$) comparing to healthy control group. The peak PSV of the hepatic artery of the infected untreated and treated with BM-MSC following ABZ were significantly differ ($P = 0.0001$). Rats treated with BM-MSC following ABZ had the highest PSV at 4th Wk PT and it was similar to that of healthy rats (Table 3).

EDV significantly decreased ($P < 0.0001$) at the 4th Wk of ABZ treatment and the 2nd and 4th Wks PT of BM-MSCs + ABZ comparing to untreated rats. TAMV was significantly higher ($P < 0.0001$) at 4th Wk PT of BM-MSC + ABZ treatment than infected untreated rats. The mean velocity was ascending linearly at 2nd and 4th Wks after treatment with ABZ alone and PT of BM-MSC + ABZ ($P = 0.0001$). S/D, G mean and G peak were significantly decreased at the 4th Wk in ABZ treated rats and at the 2nd and 4th Wks PT of BM-MSC + ABZ treatment than untreated rats. The infected untreated rats and those treated with ABZ at 2nd have the highest ($P < 0.001$) PI (Table 3).

3.2.4. Blood flow of spleen ultrasonography analysis

The picture of spleen blood flow showed a significant decrease of PSV ($P < 0.0001$), TAMV ($P < 0.001$), S/D ($P < 0.0001$) and increase of EDV, G mean and PI ($P < 0.0001$) in hydatid infected untreated rats comparing to healthy control group. It could be noticed that the blood flow velocities of the spleen represented by the PSV was the lowest ($P = 0.0001$) for the rats treated with ABZ at 2nd and Wks (Table 4). The peak systolic velocity (PSV) of the splenic artery of the healthy control rats and those infected and treated with BM-MSC + ABZ at 2nd and 4th Wks PT are the highest compared to the other treatments. The splenic end diastolic velocity (EDV) of the healthy control rats and those untreated and treated with BM-MSC + ABZ at the 2nd and 4th Wks PT are the lowest ($P = 0.0001$). TAMV of the healthy control and those treated with BM-MSC + ABZ for the 2nd and 4th Wks PT are the highest ($P = 0.001$). Though the mean velocity is not significantly influenced by treatments but rats treated with ABZ at the 2nd Wk after treatment has the lowest mean velocity (Table 4). Although the systolic/diastolic blood flow velocity of infected untreated and treated rats with ABZ at 2nd Wk are significantly the lowest ($P = 0.0001$), but the healthy control rats and those treated with BM-MSC + ABZ at 4th Wk PT are the highest. The RI of rats treated with ABZ at the 4th Wk is the lowest ($P = 0.0003$) but that at the 2nd Wk and the healthy control are the highest. The RI of the BM-MSC + ABZ group at 4th Wk PT is insignificantly low than that at 2nd Wk. The PI of healthy control and those treated with BM-MSC + ABZ at the 4th Wk are lower ($P = 0.0001$) than the other treatments. The mean splenic gradient blood pressure (G mean) of BM-MSC + ABZ treated rats at 2nd and 4th Wks were significantly lower than untreated ($P = 0.0001$). The infected untreated and those treated with ABZ at 2nd and 4th Wks have the highest G Mean (Table 4).

3.3. Gross and microscopic examination of spleen and liver

Macroscopical appearance showed white multiple nodules with different diameters; 0.5, 5, 10 mm in the liver of experimentally infected untreated rats. However, hepatomegaly and congested dark borders of the livers of ABZ treated rats at 4th Wk with white small nodules, approximately 0.5 mm in diameter. Rats treated with BM-MSC + ABZ at the 4th Wk PT showed approximately normal size and appearance of the livers with the absence of white

Table 1
Cell counting, viability, Colony forming unit-fibroblastic (CFU–F) and population doubling (PD) of rat BM-MSC.

Cell counting (cells/cm^2)	Cell viability (%)	CFU-F	Final PD score
4.68 x 10^4	92.24	14.01	65.31

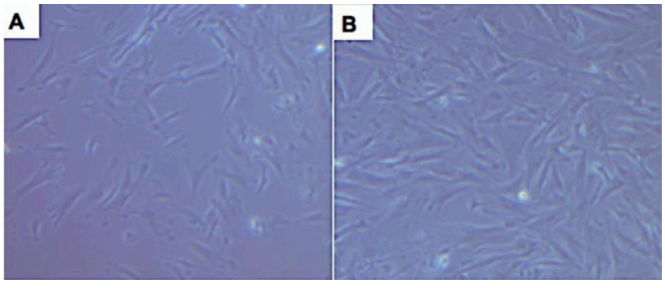

Fig. 2. Photomicrograph image showed morphology of primary layers of adherent MSCs isolated from bone marrow of rat at 50% (A) and 80% (B) confluence (×20).

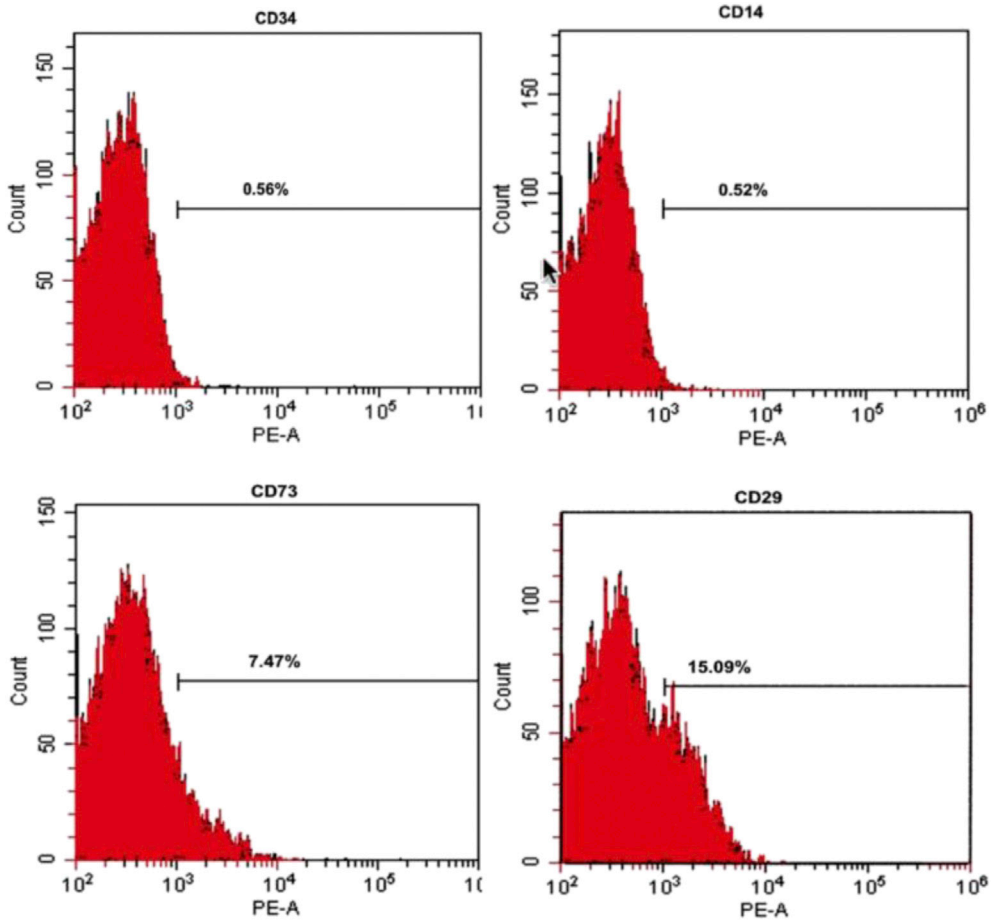

Fig. 3. Flow cytometric analysis showed that cultured immunophenotype of BM-MSC showed negative expression of CD34 and CD14 and positive expression of CD73 (7.47%), CD29 (15.09%) antibodies staining.

nodules. The spleen of healthy control rat was shown normal healthy appearance. However, spleenomegaly was shown in infected untreated and with ABZ treated rats at 4th Wk. Rats treated with BM-MSC + ABZ at 4th Wk PT showed normal appearance and size of spleen (Fig. 5).

Microscopical examination showed approximately normal hepatic structures of cells, central vein in liver section of healthy rats. However, hydatid cyst appeared in the liver of experimentally infected untreated rats with congestion of portal vein and sinusoids, biliary hyperplasia and mild biliary cirrhosis with steatosis and mononuclear cells infiltration. Moreover, liver section of ABZ treated rats at 4th Wk PT showed hydatid cyst with dilatation and congestion of central veins and sinusoids with focal area of hemorrhage. At a time, nearly normal appearance of the liver of rat treated with BM-MSC + ABZ at the 4th Wk was observed with lymphocytic infiltrates in portal area and without steatosis or necrosis. Healthy rat showed normal spleen structure, white and red pulps. White pulp expanded with a relative decrease in area of red pulp in spleen of experimentally infected untreated rats. Increase in lymphocyte cellularity in spleen of ABZ treated rats at 4th Wk was observed. Nearly normal spleen was noticed in rats at the 4th Wk PT of BM-MSC + ABZ (Fig. 6).

3.4. Humeral immune response in hydatid experimentally infected rats

Infection with hydatid protoscoleces caused elevation ($P < 0.05$) of Igs titers against HCF, HCP and HCG antigens. Results showed a significant reduction of Igs titers against HCF and HCG antigens at 4th Wk following ABZ treatment. Moreover, a significant reduction of Igs titers against HCF, HCP and HCG antigens was recorded at 4th Wk PT BM-MSCs + ABZ treatment. At 4th Wk PT of BM-MSC + ABZ treatment resulted in significant reduction ($P < 0.05$) of Igs titers against HCP antigen was recorded comparing to ABZ treatment alone. In addition, Igs titers against HCP antigen was significantly decreased ($P < 0.05$) to its normal level in BM-MSC + ABZ treated rats comparing to healthy control rats (Table 5).

Infection with hydatid caused significant elevation ($P < 0.05$) in IgM titer against HCG antigen only. However, neither ABZ treatment nor BM-MSC transplantation + ABZ treatment affected IgM titers against HCF, HCP and HCG antigens (Table 6).

Infection with hydatid caused significant elevation ($P < 0.01$) in IgG titers against HCF, HCP and HCG antigens. IgG titers against HCF and HCG significantly reduced ($P < 0.05$) at 4th Wk following ABZ treatment. However, transplantation of BM-MSC + ABZ treatment resulted in a significant decrease of IgG titers against HCF, HCP ($P < 0.01$) and HCG ($P < 0.05$) antigens at 4th Wk (Table 7).

3.5. Cell mediated immune response of hydatid experimentally infected rats (leukocytic picture, splenocytes viability and phagocytic index)

Hydatid infection resulted in a significant increase in EOS% and N% ($P < 0.05$) in untreated rats. A significant decrease was observed in EOS% at 4th Wk in rats treated with ABZ alone and at 2nd and 4th Wks PT of BM-MSC + ABZ. In addition, a significant decrease

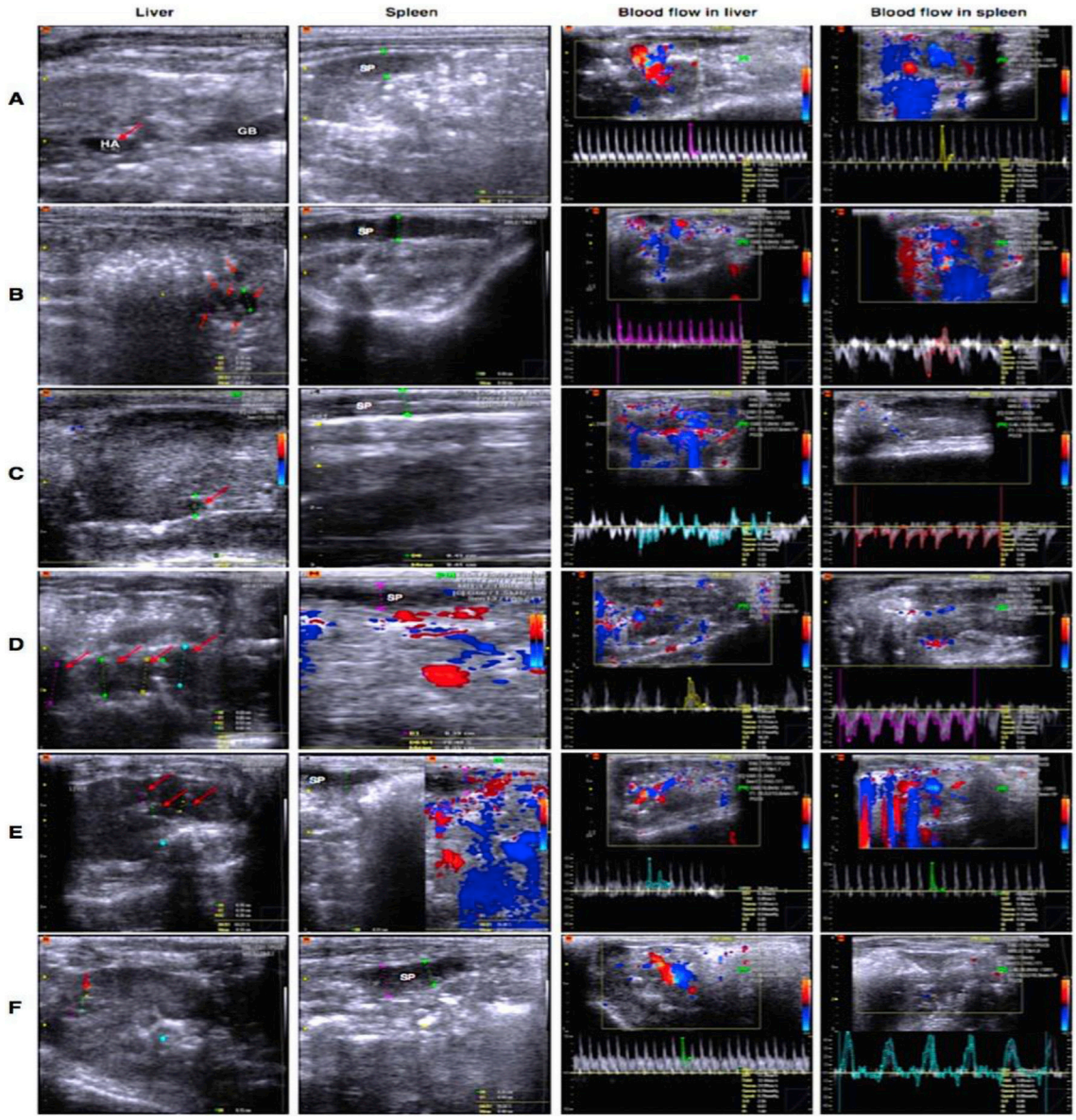

Fig. 4. Ultrasonography images of livers and spleen and their blood flow in different experimental groups. In healthy control rats the ultrasonography showed normal liver with normal hepatic artery (HA) and gall bladder (GB), normal spleen (SP) appearance with 3.1 mm diameter width and normal blood flow of liver and spleen (A). Multiple hydatid cysts (arrows) with different diameters approximately 5.9, 5.6, 5.4 and 6.6 mm were shown in liver of experimentally infected untreated rats, with a picture of low blood flow. Spleenomegaly (SP, 4.4 mm diameter width) was shown in experimentally infected untreated rats, with a picture of high blood flow (B). At the 2nd Wk following ABZ treatment, a stable hydatid cyst (arrow) in the liver approximately 5.4 mm diameter with spleenomegaly (SP, 4.1 mm diameter), low blood flow in liver and high blood flow in spleen (C). However, multiple cysts (arrows) were shown in liver at 4th Wk following ABZ treatment with diameter range 5.3, 5.1 and 6.2 mm with spleenomegaly (SP, 3.9 mm diameter), low blood flow in liver and high blood flow in spleen (D). Multiple small cysts with diameter range 1.6, 1.9 and 2 mm were shown in liver at 2nd Wk PT of BM-MSC + ABZ treatment with spleen normal size (SP, 3.5 mm diameter), normal picture of blood flow in liver and spleen (E). The cyst size decreased to diameter range 1.5 mm in liver at 4th Wk following transplantation of BM-MSC + ABZ treatment and spleen appeared in normal size (SP, 3.5 mm diameter) with normal picture of blood flow in liver and spleen (F). **A:** healthy control, **B:** untreated, **C:** ABZ 2nd Wk, **D:** ABZ 4th Wk, **E:** BM-MSCs + ABZ 2nd Wk, **F:** BM-MSC + ABZ 4th Wk.

($P < 0.05$) in N% and L% was noticed at 4th Wk PT of BM-MSC + ABZ treated rats comparing to experimentally infected untreated (Table 8). The results revealed that spleen cell viability % of infected rats was 83%. The highest spleen cell viability % (97%) was recorded at 4th Wk PT of BM-MSC + ABZ treatment (Fig. 7). The phagocytic index of *in vitro* carbon clearance test significantly decreased in hydatid experimentally infected rats. However, the phagocytic index increased significantly ($P < 0.05$) at 4th Wk in both ABZ treated group and BM-MSC + ABZ treated group. Furthermore, phagocytic index was significantly higher ($P < 0.05$) at 4th Wk in BM-MSC + ABZ treated group comparing to ABZ treated group (Fig. 7).

3.6. Th1/Th2 cytokines concentration

Serum cytokines concentration showed that TNF-α and IL-6 were significantly higher in hydatid infected untreated rats, however, IL-4 and IL-10 were significantly lower comparing to healthy control group. Transplantation of BM-MSC + ABZ treatment resulted in significant decrease of serum TNF-α ($P < 0.05$) and IL-6 ($P < 0.01$) concentrations at both the 2nd or 4th Wks PT comparing to hydatid infected untreated rats. However, IL-4 and IL-10 concentrations were significantly elevated only at 4th Wk PT of BM-MSC + ABZ treatment comparing to untreated rats (Table 9).

Table 2
Morphometric ultrasonography analysis.

Parameters	Healthy control	Hydatid infected rats				
		Untreated	ABZ		BM-MSC + ABZ	
			2nd Wk	4th Wk	2nd Wk	4th Wk
Spleen length (mm)	5.321 ± 1.418	20.0[a] ± 3.108	18.0 ± 1.276	17.211 ± 1.386	6.728[*] ± 0.931	6.353[*] ± 0.698
Spleen width (mm)	3.111 ± 0.286	6.719[a] ± 0.281	5.491 ± 0.243	6.351 ± 0.318	3.709[*] ± 0.221	3.520[*] ± 0.182
Average cystic diameter in uni-cyst liver (mm)	0.00	5.882 ± 0.387	5.117 ± 0.222	5.536 ± 0.317	1.301[*] ± 0.234	1.247[*] ± 0.276
Average cystic diameter in Multi-cyst liver (mm)	0.00	6.621 ± 0.251	5.69 ± 0.327	5.436 ± 0.342	1.813[*] ± 0.174	1.512[*] ± 0.163

All data expressed as Mean ± SE.
[a] are significantly different than healthy control at $P < 0.05$.
[*] significantly different than infected untreated at $P < 0.05$.

Table 3
Blood flow of liver measuring the peak systolic velocity (PSV), end diastolic velocity (EDV), time average maximum velocity (TAMV), velocity mean (V), G mean, G peak, systolic/diastolic (S/D), resistance index (RI) and pulsatility index (PI).

Parameters	Healthy control	Hydatid infected rats					P-value
		Untreated	ABZ		BM-MSC + ABZ		
			2nd Wk	4th Wk	2nd Wk	4th Wk	
PSV (cm/s)	43.67[e] ± 0.38	18.67[a] ± 0.61	21.67[b] ± 0.51	32.01[c] ± 0.65	34.33[d] ± 0.51	43.01[e] ± 0.65	0.0001
EDV (cm/s)	4.67[a] ± 0.14	8.01[c] ± 0.65	8.02[c] ± 0.62	6.05[b] ± 0.25	5.06[ab] ± 0.24	5.33[ab] ± 0.37	0.0001
TAMV (cm/s)	7.33[bc] ± 0.28	5.01[a] ± 0.26	5.07[a] ± 0.04	7.33[bc] ± 0.14	6.67[b] ± 0.38	8.09[c] ± 0.25	0.0001
Mean velocity (cm/s)	18.33[e] ± 0.28	10.33[a] ± 1.38	12.33[b] ± 0.38	15.02[c] ± 0.43	16.33[d] ± 0.38	17.67[e] ± 0.14	0.0001
S/D	0.05[a] ± 0.00	0.26[c] ± 0.01	0.28[c] ± 0.03	0.19[b] ± 0.01	0.07[a] ± 0.00	0.06[a] ± 0.00	0.0001
RI	0.78 ± 0.01	0.82 ± 0.03	0.76 ± 0.05	0.79 ± 0.02	0.79 ± 0.02	0.78 ± 0.05	0.81
PI	1.59[a] ± 0.07	2.11[cd] ± 0.17	2.30[d] ± 0.17	1.85[ab] ± 0.06	1.99[bcd] ± 0.08	1.61[ab] ± 0.14	0.001
G Mean (mmHg)	0.27[a] ± 0.02	0.88[d] ± 0.03	0.89[d] ± 0.02	0.53[c] ± 0.01	0.39[b] ± 0.02	0.26[a] ± 0.01	0.0001
G Peak (mmHg)	4.35[a] ± 0.28	6.11[b] ± 0.29	7.14[c] ± 0.48	5.78[b] ± 0.30	5.75[b] ± 0.08	4.71[a] ± 0.19	0.0001

All data expressed as Mean ± SE.
Means with different superscripts within the same row are significantly differ.

Table 4
Blood flow of spleen measuring the peak systolic velocity (PCV), end diastolic velocity (EDV), time average maximum velocity (TAMV), velocity mean (V), G mean, G peak, systolic/diastolic (S/D), resistance index (RI) and pulsatility index (PI).

Parameters	Healthy control	Hydatid infected rats					P-value
		Untreated	ABZ		BM-MSC + ABZ		
			2nd Wk	4th Wk	2nd Wk	4th Wk	
PSV (cm/s)	44.29[d] ± 0.68	32.35[b] ± 0.84	29.59[a] ± 0.39	29.48[a] ± 0.32	39.40[c] ± 0.75	41.14[c] ± 0.73	0.0001
EDV (cm/s)	4.98[a] ± 0.33	6.67[b] ± 0.20	7.08[b] ± 0.31	6.46[b] ± 0.22	4.72[a] ± 0.08	4.75[a] ± 0.29	0.0001
TAMV (cm/s)	5.91[b] ± 0.27	4.70[a] ± 0.16	4.85[a] ± 0.40	4.80[a] ± 0.04	5.59[b] ± 0.19	5.61[b] ± 0.22	0.001
V Mean (cm/s)	11.14[b] ± 0.36	11.13[b] ± 1.29	10.09[a] ± 0.27	10.86[ab] ± 0.16	11.14[b] ± 0.39	11.18[b] ± 0.41	0.14
S/D	0.17[c] ± 0.00	0.13[a] ± 0.00	0.12[a] ± 0.00	0.16[b] ± 0.00	0.16[b] ± 0.01	0.17[c] ± 0.00	0.0001
RI	0.83[bc] ± 0.03	0.76[ab] ± 0.04	0.87[c] ± 0.02	0.69[a] ± 0.02	0.79[bc] ± 0.02	0.75[ab] ± 0.04	0.003
PI	3.64[a] ± 0.13	6.16[c] ± 0.23	6.84[c] ± 0.25	4.19[ab] ± 0.29	4.75[b] ± 0.35	3.89[a] ± 0.09	0.0001
G Mean (mmHg)	0.46[a] ± 0.02	0.71[c] ± 0.04	0.77[c] ± 0.02	0.73[c] ± 0.03	0.61[b] ± 0.03	0.58[b] ± 0.04	0.0001
G Peak (mmHg)	6.06 ± 0.37	6.14 ± 0.16	6.13 ± 0.26	6.08 ± 0.23	5.60 ± 0.26	5.88 ± 0.05	0.60

All data expressed as Mean ± SE.
Means with different superscripts within the same row are significantly differ.

4. Discussion

Immune defense mechanism to solve problems of cystic hydatidosis is in the mind of scientists. Effective treatments as well as well-designed immunomodulation are poor and the trials that could guide therapy are overdue [3]. Several problems are involved, firstly, *Echinococcus* organisms, are able to modulate host anti-parasite immune responses [5]. Secondary, the usage of both shielding and down-regulatory tools by the parasites to protect their own presence. These tools are their antigens; outer tegumental coat and continuously released excretory/secretory products [5]. This obstacle limits the effectiveness of parasite control programs [4]. The program is stagnant use of albendazole (ABZ) as anthelmintic treatment [6]. Therefore, there is a massive requirement for other tool for hydatid disease control [7]. The use of BM-MSC for hydatid experimentally infected rat in the present study hoping to solve this problem and consequently, open the road to be used in human and large animals. The underlining mechanism of using cell therapy in this work is to modulate immune responses against cystic antigens by modulating regulatory B and T cells and regenerate injured tissues.

Counting of 80% confluent BM-MSC was 4.68×10^4 cells/cm^2 with 92.24% viability. A continuous cell culture assay indicates that BM-MSC acquired number of population doublings. Final

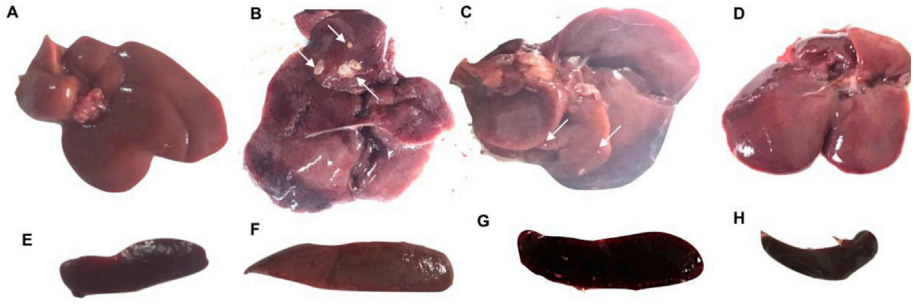

Fig. 5. Livers and spleen of healthy and hydatid experimentally infected untreated and treated rats. Normal healthy appearance of liver of healthy control rat (A). White Multiple nodules (arrows) with different diameters; 0.5, 5, 10 mm, were shown in the liver of experimentally infected untreated rats (B). Hepatomegaly and congested dark borders of the livers of ABZ treated rats at 4th Wk PT with white small nodules (arrows), approximately 0.5 mm in diameter (C). Approximately normal size and appearance of the livers of rats treated with BM-MSC + ABZ at the 4th Wk PT with the absence of white nodules (D). Normal healthy appearance of spleen of healthy control rat (E). Spleenomegaly was shown in infected untreated rats (F). Spleenomegaly was shown in infected rats treated with ABZ at 4th Wk (G). Normal appearance and size of spleen of rats treated with BM-MSC + ABZ at 4th Wk PT (H).

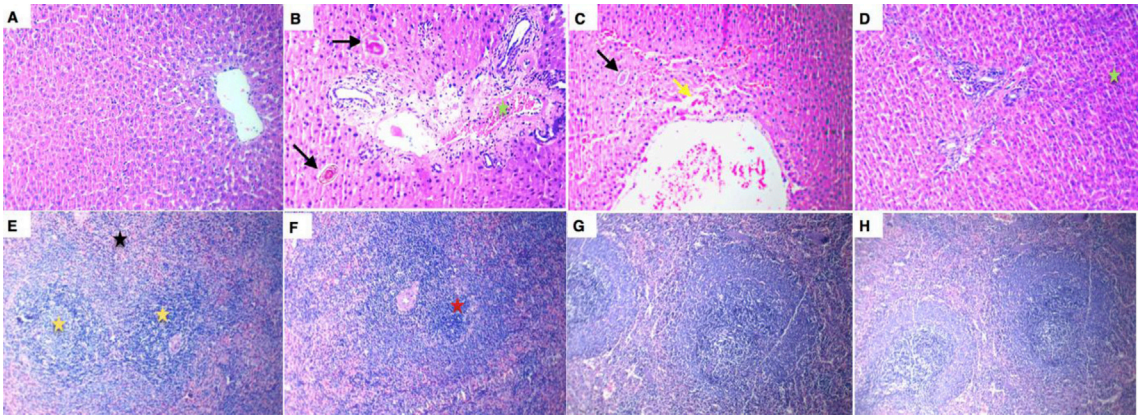

Fig. 6. Liver section of healthy rat showing approximately normal hepatic structures of cells, central vein (A). Hydatid cyst (black arrows) appeared in the liver of experimentally infected untreated rat with congestion of portal vein and sinusoids, biliary hyperplasia and mild biliary cirrhosis (green asterisk) with steatosis and mononuclear cells infiltration (yellow arrow) (B). Liver section of ABZ treated rat at 4th Wk PT showed hydatid cyst (black arrow) with dilatation and congestion of central veins and sinusoids with focal area of hemorrhage (yellow arrow) (C). Nearly normal appearance of the liver of rat treated with BM-MSC + ABZ at the 4th Wk with lymphocytic infiltrates (green asterisk) in portal area and without steatosis or necrosis (D). Normal spleen structure, white (yellow asterisk) and red (black asterisk) pulp of healthy rat (E). Expansion of white pulp (red asterisk) with a relative decrease in area of red pulp in spleen of experimentally infected untreated rat (F). Increase in lymphocyte cellularity in spleen of ABZ treated rat at 4th Wks (G). Nearly normal spleen of BM-MSC + ABZ treated rat at the 4th Wk PT (H) (H&E ×40).

Table 5
Total immunoglobulins (Igs) against HCF, HCP and HCG antigens in serum of hydatid experimentally infected rats (OD).

Parameters	Healthy control	Hydatid infected rats				
		Untreated	ABZ		BM-MSC + ABZ	
			2nd Wk	4th Wk	2nd Wk	4th Wk
HCF	0.122 ± 0.03	0.738[a] ± 0.16	0.476 ± 0.06	0.311[*] ± 0.01	0.481 ± 0.04	0.326[*] ± 0.02
HCP	0.213 ± 0.06	0.726[a] ± 0.17	0.578 ± 0.05	0.532 ± 0.06	0.537 ± 0.05	0.271[*] ± 0.05
HCG	0.131 ± 0.04	0.794[A] ± 0.14	0.593 ± 0.07	0.396[*] ± 0.03	0.641 ± 0.05	0.384[*] ± 0.02

All data expressed as Mean ± SE.
[a] and [A] significantly different than their corresponding healthy control at $P < 0.05$ and $P < 0.01$ respectively.
[*] significantly different than their corresponding untreated at $P < 0.05$.
HCF: hydatid cyst fluid, HCP: hydatid cyst protoscolex, HCG: hydatid cyst germinal layer.

population doublings score was 65.31 that indicated attachment, proliferation, and self-renewal capacity of BM-MSC. BM-MSC was expressed markers by flow cytometric analysis, particularly, 0.56% of BM-MSC expressed CD34, a specific marker of hematopoietic stem and endothelial cells, while 0.52% of BM-MSC expressed CD14. However, BM-MSC expressed CD73, and CD29 (7.47% and 15.09% respectively). These results indicated that the isolated BM-MSC was positively expressed CD marker for MSCs and negatively for hematopoietic stem cell markers as nearly described by The Mesenchymal and Tissue Stem Cell Committee of International Society for Cellular Therapy [37].

Rats were followed up by ultrasound, gross anatomy, pathological and immunological examinations. Ultrasonography is a sensitive way for the diagnosis of hepatic hydatid cyst; therefore, as an objective non-invasive practical tool, ultrasonography alone or in combination with testing of biochemical parameters reflecting

Table 6
Immunoglobulin M (IgM) against HCF, HCP and HCG antigens in serum of experimentally infected rats (OD).

Parameters	Healthy control	Hydatid infected rats				
		Untreated	ABZ		BM-MSC + ABZ	
			2nd Wk	4th Wk	2nd Wk	4th Wk
HCF	0.031 ± 0.007	0.053 ± 0.01	0.082 ± 0.02	0.079 ± 0.02	0.077 ± 0.02	0.054 ± 0.01
HCP	0.012 ± 0.003	0.023 ± 0.005	0.027 ± 0.006	0.025 ± 0.007	0.023 ± 0.004	0.028 ± 0.007
HCG	0.042 ± 0.01	0.149[a] ± 0.04	0.084 ± 0.02	0.081 ± 0.02	0.059 ± 0.01	0.067 ± 0.01

All data expressed as Mean ± SE.
[a] significantly different than their corresponding healthy control at $P < 0.05$.
HCF: hydatid cyst fluid, HCP: hydatid cyst protoscolex, HCG: hydatid cyst germinal layer.

Table 7
Immunoglobulin G (IgG) against HCF, HCP and HCG antigens in serum of experimentally infected rats (OD).

Parameters	Healthy control	Hydatid infected rats				
		Untreated	ABZ		BM-MSC + ABZ	
			2nd Wk	4th Wk	2nd Wk	4th Wk
HCF	0.112 ± 0.03	0.431[A] ± 0.05	0.452 ± 0.02	0.287[*] ± 0.02	0.433 ± 0.02	0.211[**] ± 0.04
HCP	0.131 ± 0.04	0.648[A] ± 0.15	0.518 ± 0.04	0.573 ± 0.03	0.524 ± 0.02	0.135[**] ± 0.02
HCG	0.102 ± 0.03	0.631[A] ± 0.12	0.493 ± 0.06	0.252[*] ± 0.07	0.441 ± 0.11	0.243[*] ± 0.04

All data expressed as Mean ± SE.
[A] significantly different than their corresponding healthy control at $P < 0.01$.
[*] and [**] significantly different than their corresponding untreated at $P < 0.05$ and $P < 0.01$ respectively.
HCF: hydatid cyst fluid, HCP: hydatid cyst protoscolex, HCG: hydatid cyst germinal layer.

Table 8
Eosinophils (EOS), Neutrophil (N), lymphocyte (L) and N/L ratio of hydatid experimentally infected rats.

Parameters	Healthy control	Hydatid infected rats				
		Untreated	ABZ		BM-MSC + ABZ	
			2nd Wk	4th Wk	2nd Wk	4th Wk
EOS%	2.45 ± 0.13	8.46[A] ± 1.25	6.44 ± 0.38	4.58[*] ± 0.62	4.52[*] ± 0.56	3.16[*] ± 0.65
N%	70.33 ± 2.34	78.12[a] ± 2.06	73.26 ± 5.18	72.09 ± 4.86	74.23 ± 3.97	68.16[*] ± 3.15
L%	22.61 ± 2.96	21.48 ± 4.26	23.72 ± 2.74	28.91 ± 2.55	25.77 ± 4.23	31.84[*] ± 3.56
N/L ratio	3.19 ± 0.97	3.65 ± 0.04	3.12 ± 0.23	2.86 ± 0.75	2.99 ± 0.69	2.20[*] ± 0.04

All data expressed as Mean ± SE.
[a] and [A] significantly different than their corresponding healthy control at $P < 0.05$ and $P < 0.01$ respectively.
[*] significantly different than their corresponding untreated at $P < 0.05$.

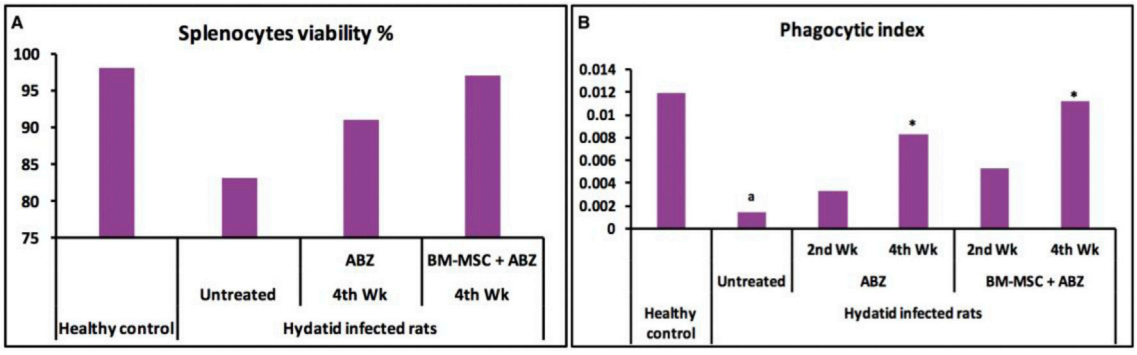

Fig. 7. Splenocytes viability % (A) and phagocytic index (B) of healthy control, hydatid experimentally infected and ABZ and BM-MSC treated rats. [a] significantly different than their corresponding healthy control at $P < 0.01$. [*] significantly different than their corresponding untreated at $P < 0.05$.

liver function could be helpful for diagnosis of hydatidosis in liver [38]. In this study, ultrasonographic aspects showed multiple hydatid cysts with a picture of low blood flow in the liver and spleenomegaly with a picture of high blood flow of hydatid experimentally infected rats. Low PSV, high EDV, low V mean, high S/D, high G mean and high RI and PI were observed in infected rats. The average cyst diameter was approximately 5.9, 5.6, 5.4 and 6.6 mm. These findings are in agreement with previous study [31] that indicating a significant expansion in the diameter by time after 6 months of infection. In this study, ultrasound measured a

Table 9
Th1 cytokines (TNF-α, IL-6) and Th2 cytokines (IL-4, IL-10) of hydatid experimentally infected rats (ng/ml).

Parameters	Healthy control	Hydatid infected rats				
		Untreated	ABZ		BM-MSC + ABZ	
			2nd Wk	4th Wk	2nd Wk	4th Wk
TNF-α	8.350 ± 1.46	14.576[a] ± 1.11	9.381 ± 1.17	9.523 ± 1.32	8.301[*] ± 1.77	7.44[**] ± 1.86
IL-6	9.775 ± 1.05	13.963[a] ± 1.32	12.237 ± 1.31	11.752 ± 1.33	9.554[*] ± 1.02	6.280[*] ± 1.45
IL-4	11.531 ± 1.83	6.115[a] ± 1.08	7.497 ± 1.45	7.905 ± 1.09	9.184 ± 1.15	12.137[*] ± 2.28
IL-10	11.864 ± 1.27	7.518[a] ± 1.12	9.851 ± 1.80	9.053 ± 1.12	11.210 ± 1.27	12.245[*] ± 1.41

All data expressed as Mean ± SE.
[a] significantly different than their corresponding healthy control at $P < 0.05$.
[*] and [**] significantly different than their corresponding untreated at $P < 0.05$ and $P < 0.01$ respectively.

detectable stable hydatid cyst in the liver approximately 5.4–6.2 mm diameter range with spleenomegaly, low blood flow in liver and high blood flow in spleen was observed at the 2nd and 4th Wks following ABZ treatment. Multiple small cysts with diameter range 1.6, 1.9 and 2 mm were shown in liver at 2nd Wk PT of BM-MSC following ABZ treatment. This cyst size decreased to diameter range 1.5 mm at 4th Wk PT of BM-MSC following ABZ treatment and spleen appeared in normal size with normal picture of blood flow in liver and spleen. These findings indicated that hydatid cysts caused some liver features alterations that could be regenerated by BM-MSC transplantation.

A picture of low blood flow of liver was observed in infected rats by means of significant low PSV, high EDV, low V mean, high S/D, high G mean and high RI and PI comparing to healthy control group. At the 2nd and 4th Wks following transplantation of BM-MSC + ABZ treatment, PSV increased while EDV decreased comparing to infected rats. TAMV was significantly higher at 4th Wk following transplantation of BM-MSC + ABZ treatment than infected rats. S/D and G mean were significantly decreased 2nd and 4th Wks following transplantation of BM-MSC + ABZ treatment than infected rats. The picture of spleen blood flow showed a significant increase in PSV, S/D, G mean and PI in hydatid infected rats comparing to healthy control group. However, PSV significantly decreased and EDV significantly increased at 2nd and 4th Wks following transplantation of BM-MSC + ABZ treatment comparing to infected rats. Moreover, S/D significantly increased ($P < 0.05$) and PI significantly decreased at the 4th Wk following transplantation of BM-MSC + ABZ treatment comparing to infected rats.

The gross anatomy showed white multiple nodules with different diameters; 0.5, 5, 10 mm in the liver and spleenomegaly in hydatid experimentally infected rats. However, hepatomegaly and congested dark borders of the livers were noticed in ABZ treated rats at 4th Wk with white small nodules, approximately 0.5 mm in diameter. Rats treated with BM-MSC following ABZ administration showed approximately normal size and appearance of the livers with the absence of white nodules at the 4th Wk PT. Spleenomegaly was shown in infected untreated and in ABZ treated rats at 4th Wk that reflected protoscolex immune reaction [25]. However, transplantation of BM-MSC following ABZ administration resulted in normal appearance and size of spleen of rats at 4th Wk PT.

Microscopical finding of the rats' livers and spleen revealed parasitism correlated pathological features. After infection, hydatid cysts appeared in the liver and the protoscolices congested the portal vein and sinusoids. They caused biliary hyperplasia and mild biliary cirrhosis with steatosis and mononuclear cells infiltration. Similar pathological features were recorded in rats [31]. **Kodama et al** [39] also reported the appearance of cysts and central necrosis with granulation, fibrosis, and calcification which were the main constituents of liver hydatid cyst in human. These results also were confirmed previously in mice animal model [25] who recorded that the protoscolices migrated through blood flow to the portal vein to settled in the liver and developed into hepatic hydatid cysts, similar to the route and course of the natural infection. The rats' liver also showed protective immune reactions, such as mononuclear cells infiltration and fibrosis capsules.

Moreover, liver section of ABZ treated rats at 4th Wk showed hydatid cyst with dilatation and congestion of central veins and sinusoids with focal area of hemorrhage. It was noticed that chemotherapy was more effective against small cysts, might be due to thin walls of these cysts [40]. It was confirmed in patients with high risk for surgery, multiple peritoneal cysts, cysts in multiple organs to avoid secondary hydatidosis after surgical discharge [41]. In addition, dead protoscolices resulted in focal degeneration and necrosis; and the liver responded by a dilatation of central veins [25]. At a time, nearly normal appearance of the liver of rat at the 4th Wk PT of BM-MSC following ABZ administration was observed with lymphocytic infiltrates in portal area without steatosis or necrosis. Histopathological features also revealed an expansion of spleen white pulp with a relative decrease in area of red pulp in experimentally infected untreated rat. In addition, an elevation in lymphocyte cellularity in spleen of ABZ treated rat at 4th Wk was observed. On the other hand, nearly normal spleen was noticed in rat at the 4th Wk PT of BM-MSC following ABZ administration.

This study experimentally manipulated the effect of hydatid cyst on immune parameters to assess the value of humeral and cell mediated immune response. The humeral immune response was assessed by determination of Igs, IgM and IgG antibodies while the cell mediated immune response was demonstrated by eosinophils, neutrophils and lymphocytes count and phagocytic index. In this study, when hydatid cyst developed in the liver of experimentally infected rats, Igs and IgG response to HCF, HCP and HCG were significantly elevated as a result of persistent infection which leads to release of antibodies against it. However, infection with hydatid caused significant elevation in IgM response to HCG only. This result might be due to the time of samples collection and estimation of IgM which was at the 8th Wk post infection whereas IgM disappeared after the 4th Wk post infection. The rats produced the host immune response following injection of protoscolices [42]. Subsequently, cyst membranes and capsules were developed by the protoscolices to protect the parasite from the host immune invasion [25]. The host-parasite humeral immune reaction was reflected by release of Igs as well as IgG could be used as indirect indicator to estimate the hydatid cyst capacity and the parasites load [42]. The earliest IgG response to hydatid cyst fluid (HCF) and germinal layer antigens (HCG) appeared previously in mice and sheep, respectively [43]. These antibodies played a key role in the eradication of the parasite and were essential to the defensive immune reaction against cyst infection. In the early infection, the responses of antibodies against protoscolex antigen (HCP) are moderately weak and usually overdue and then they are augmented later [42].

About 8- to 10- Wks post infection, cyst growth was continued and complex echinococcal antigens were discharged from the cyst to stimulate complex immune reactions. At this stage, the parasite produced considerable amounts of antigens that trigger immune response modulation, by elevation of IgG, specially IgG1, and IgM levels that may be of value for both parasite and host [8]. In this investigation, ABZ treatment accompanied with significant decrease in Igs and IgG titers against HCF and HCG only at 4th Wk following treatment. However, Igs titer against HCF, HCP and HCG was significantly decreased at the 4th Wk PT of BM-MSC following ABZ treatment. Interestingly, the transplantation of BM-MSC after ABZ treatment resulted in reduction of Igs response to HCP to normal level as that of healthy control. BM-MSC might affect protoscolices resulting in a decrease in the antibody titer against them. From these results, it was observed that transplantation of BM-MSC following ABZ treatment resulted in significant reduction of Igs anti-HCP comparing to ABZ treatment alone. It was clear that the picture of IgG and IgM titer in ABZ treated rats had a similar pattern to that of rats treated by BM-MSC transplantation at 2nd Wk following ABZ administration. Neither ABZ nor BM-MSC combination affect IgM titer.

It was previously observed that the core characteristics of MSC are their regenerative and immunomodulation potentiality that enhances and modulates both adaptive and innate immune responses [44]. This function occurred due to its close association with blood vessels which provides metabolic signals to immune system, as well as secretion of humoral factors and cytokines [45] or paracrine mechanisms [46]. These properties have made MSC a potential therapeutic choice for immune and inflammatory disorders and repair and regenerative processes [47]. The granular formation around the parasitic lesion, in many helminthic infections, is a major component of effective containment of the invader. This construction is a response by neutrophils and macrophages towards a group of exotic organisms or material and is mainly due to a Th1 response [5]. The parasites have to avoid being destroyed by the hosts defense mechanisms by sheltering their own existence and reproduction without causing unnecessary harm to their hosts [5]. Infection resulted in elevation of Th1 cytokines (TNF-α, IL-6) which might be due to liver necrosis resulting from infection. On the other hand, Th2 cytokines (IL-4 and IL-10) decreased in infected rats. This reduction in Th2 cytokines might be due to infection which stimulated cellular immune response more than humeral response. After transplantation of BM-MSC + ABZ treatment serum TNF-α and IL-6 concentrations were reduced at both the 2nd or 4th Wks. However, IL-4 and IL-10 concentrations were significantly elevated only at 4th Wk PT of BM-MSC following ABZ treatment. It could be suggested that by relieve IL-10 increased to decrease TNF-α and increase IL-4 resulting in stimulation of humeral immune response. A shifting in the cytokine profile from Th1 to Th2 variables was reported during the late chronic stage of E. multilocularis infection [48,49]. Moreover, inhibition of dendritic cells function and activity, a deficiency of antigen manifestation might cause shifting of T-cells to the down regulating T-regulatory response. The initial response is of the Th1-type, it progressively shifts into a Th2 response [49]. This swing in the cytokine profile could be host protective by reducing inflammation, but it can be also less effective at parasitic infection control [5]. The proliferative larval stage is continuing resulting in additional cysts expansion and growth, that may invade other tissues. During this stage, the larva has an outer laminated layer (LL), for the protection from host immune system. This LL is composed of a broad carbohydrate component known as Em2 (G11) that has weak antigenic characteristic in the stimulating of T-cell response [50]. All of these factors might consulate or inhibit the host immune response, and modify it in a manner by which the parasite can survive easily [5]. Chronic Echinococcus infection is associated with elevated level of IL-10,[8] a mediator related to the effector responses immuno-regulation and eventually inflammatory responses cessation. IL-10 also regulates leukocytes growth and differentiation including regulatory T cells, which may prominently in the tolerance in vivo. At this point, ineffective cellular immune response to invade tissue of cyst takes place [43]. It looks clear that the parasite has established protective strategies from the immune system with low effectiveness of Th1/Th2 balance shifting into Th2-response, and final to a down-regulatory T cells. This shifting could be a result of lack of stimulation on the immune cells, hence the parasite not only actively inhibits the immune system, but also develops its immune mechanisms against it [5]. Recently, **Wang et al** [46] reported that uncontrollable systemic inflammation was accompanying to acute liver failure. There was elevation of Th1 pro-inflammatory cytokines while Th2 anti-inflammatory cytokines decreased. It was suggested that acute liver failure is a strong cellular immune response that are reliable with the clinical symptoms, and conform the role for the immune microenvironment. Besides improving liver function as indicated by restoring activity of ALT and AST, MSC also produce the anti-inflammatory cytokine IL-10 suggesting a critical role in the treatment of acute liver failure with MSC. IL-10 played a major role in inflammatory response reduction by reducing the pro-inflammatory cytokines expression. Therefore, MSC transplantation could recover acute liver failure by keeping higher levels of IL-10 for longer time [46]. Studies of **Gazdic et al** [51] indicated that MSC therapy may relive inflammation of liver, and consequently improve hepatocytes regeneration, which could be a hopeful strategy for immune mediated liver damages. Nowadays, MSC is an instinctive response to the inflammation and immune-modulation by releasing soluble factors and/or by contacting cellular signaling [52]. High-stress state of liver infection may lead to a great number of antigens, sequences of immune cells, inflammatory agents and chemokines. The imbalance of liver immune microenvironment can lead to excessive activation of immune cells that affect immune damage reactions to liver [53]. The cytokine profile can simulate the MSC immunomodulation effect [54], therefore, MSC repaired liver abnormalities through IL-10 production [46].

Hydatid infection resulted in a significant increase in neutrophils in infected untreated group. A significant decrease in neutrophils and lymphocytes percent was observed at 4th Wk PT of BM-MSC combined with ABZ treatment comparing to experimentally infected untreated group. The results revealed that spleen cell viability % of infected rats were 83%. The highest spleen cell viability (97%) was recorded at 4th Wk PT of BM-MSC combined with ABZ treatment. The phagocytic index of *in vitro* carbon clearance test was significantly decreased in hydatid experimentally infected rats. However, the phagocytic index increased significantly at 4th Wk PT in both ABZ treated group and rats treated with BM-MSC transplantation following ABZ administration. Furthermore, phagocytic index was significantly higher at 4th Wk PT in rats treated with BM-MSC transplantation following ABZ administration comparing to ABZ treated group. As previously recorded, MSC stimulated T cells expansion and activation along with its subgroup *in vitro* as well as in an animal model [55,56]. It regulates growth, differentiation and viability of the immune system cells including B and T cells and NK cells, hence affecting inflammatory responses [57]. MSCs mediated the cell cycle arrest at G0/G1 and consequently prevent their differentiation into plasma cells and forming subsequent Ig [58]. This above-mentioned mechanism can be the probable cause of cell–cell contact of MSC with T-helper cells and mediators secretion [45]. By ultrasonography analysis, stable single or multiple hydatid cysts were recorded in the liver besides spleenomegaly with low blood flow in liver and high blood flow in spleen at 2nd and 4th Wks following ABZ treatment. Multiple and single small

cysts were noted in liver following transplantation of BM-MSC following ABZ treatment at 2nd and 4th Wks respectively with normal spleen and normal picture of blood flow in liver and spleen.

It was believed that, BM-MSC transplantation following ABZ administration can regenerate injured liver tissue without complete disappearance of hydatid cyst. In addition, it can modulate host protective humeral immune responses against hydatid cyst antigens by modifying the immunoglobulins response against the different hydatid isolated antigens nearly to the normal level as that of healthy control. Modification of cellular immune responses was also occurred by increasing the spleen cell viability and the phagocytic index. Cytokines profile of infected rats was reversed from elevated Th1 (TNF-α and IL-6) towards Th2 (IL-4) and IL-10 that indicated a downregulation of hydatid infection inflammatory state. Interestingly, it can be concluded that BM-MSC cell therapy is recommended as a good candidate in hydatid infection in human and animals.

Conflict of interest

The authors declare that there is no conflicts of interest.

Acknowledgements

This work was financially supported by the National Research Centre, Egypt through research project No. 11020203.

References

[1] Shimeles A, Awole M. Crossectional. Study on the prevalence and economic significance of hydatidosis in slaughtered ruminants at Debre Zeit Elfora export abattoir Oromia Region Eastern Showa Zone, Ethiopia. Biomed J Sci Tech Res 2018;3(3):1–9.
[2] Agudelo HNI, Brunetti E, McCloskey C. Cystic echinococcosis. J Clin Microbiol 2016;54:518–23.
[3] Nabarro LE, Amin Z, Chiodini PL. Current management of cystic echinococcosis: a survey of specialist practice. Clin Infect Dis 2015;60:721–8.
[4] Moreau E, Chauvin A. Immunity against helminths: interactions with the host and the intercurrent infections. J Biomed Biotechnol 2010;3:428593.
[5] Viktor A. Echinococcus multilocularis immunomodulatory strategies in the intermediate host. Vet. program. 2012:71.
[6] Shams UB, Sajad HA, Ajaz AM, et al. Role of albendazole in the management of hydatid cyst liver. Saudi J Gastroenterol 2011;17(5):343–7.
[7] Abo-Aziza AMF, Zaki AA. Immunomodulation and regenerative potentiality of hepatogenic bone marrow mesenchymal stem cells (BM-MSC) combined with praziquantel on hydatid induced hepatic cyst. J Bacteriol Parasitol 2018;9:27.
[8] Zhang W, Allen GR, Donald PM. Mechanisms of immunity in hydatid disease: implications for vaccine development. J Immunol 2008a;181:6679–85.
[9] Gebreyohannes M, Wondie M. Hydatidosis: prevalence and economic significance in cattle slaughtered at Diredawa Municipal abattoir, Ethiopia. Int J Agro Vet Med Sci (IJAVMS) 2014;8(3):64–80.
[10] Tsuchiya A, Yuichi K, Shunzo I, et al. Clinical trials using mesenchymal stem cells in liver diseases and inflammatory bowel diseases. Inflamm Regen 2017;1(37):16.
[11] Botezatu C, Bogdan M, Traian P. Hepatic hydatid cyst – diagnose and treatment algorithm. J Med Life 2018;11(3):203–9.
[12] Sokouti M, Ramin S, Saeid P, et al. A systematic review and meta-analysis on the treatment of liver hydatid cyst using meta-MUMS tool: comparing PAIR and laparoscopic procedures. Arch Med Sci 2019;15(2):284–308.
[13] Shiota G, Itaba N. Progress in stem cell-based therapy for liver disease. Hepatol Res 2016:1–15.
[14] Eom YW, Shim KY, Baik SK. Mesenchymal stem cell therapy for liver fibrosis. Korean J Intern Med 2015;30:580–9.
[15] Yamaza T, Fatima SA, Ratih Y, et al. In vivo hepatogenic capacity and therapeutic potential of stem cells from human exfoliated deciduous teeth in liver fibrosis in mice. Stem Cell Res Ther 2015;6:171.
[16] Bi H, Leiguo M, Ruiping C, et al. Liver extracellular matrix promotes BM-MSCs hepatic differentiation and reversal of liver fibrosis through activation of integrin pathway. J Tissue Eng Regenerat Med 2017;11(10):2685–9.
[17] Squillaro T, Gianfranco P, Umberto G. Clinical trials with mesenchymal stem cells: an update. Cell Transplant 2016;25:829–48.
[18] Dave M, Jaiswal P, Cominelli F. Mesenchymal stem/stromal cell therapy for inflammatory bowel disease: an updated review with maintenance of remission. Curr Opin Gastroenterol 2017;33:59–68.
[19] Elwakeel EE, Mohamed AZ. The Hepatotoxic effect induced by methotrexate therapy and protective role of bone marrow-derived mesenchymal stem cells in adult male albino rats. Histological and ultrastructural study. Jounal Am Sci 2018;14(5).
[20] Stephen J, Elena LB, David C, Alasdair RF, Juraj P, John DMC. Mesenchymal stromal cells as multifunctional cellular therapeutics – a potential role for extracellular vesicles. Transfus Apher Sci 2016;55:62–9.
[21] Tabar HGR, Borji H. Antibody responses to hydatid cyst in experimentally infected lambs. World Appl Sci J 2010;8(8):1001–6.
[22] Nouroozi RV, Moulood VN, Masoumeh A. Determination of protein concentration using Bradford microplate protein quantification assay. Int Electron J Med 2015;4(1):11–7.
[23] Innocenti L, Masetti M, Macchioni G, Giorgi F. Larval salivary gland proteins of the sheep nasal bot fly, (*Oestrus ovis* L.), are major immunogens in infested sheep. Vet Parasitol 1995;60:273–82.
[24] Ouchterlony O. Antigen-antibody reaction in gels, types of reactions in coordinated system of diffusion. Acta Pathol Microbiol Scand 1953;32:231.
[25] Zhang R, Chen X, Hao W. Improved experimental model of hepatic cystic hydatid disease resembling natural infection route with stable growing dynamics and immune reaction. World J Gastroenterol 2017;23(45):7989–99.
[26] Lee SO, Sang-Ho C, Chan-Lan K, et al. Enhanced adipogenic differentiation of bovine bone marrow- derived mesenchymal stem cells. J Appl Anim Res 2015;431:15–21.
[27] Al-Mutairi KSH, ALmundarij TI, Zaki AA. Osteogenic/adipogenic differentiation of intact and ovariectomized young and adult female rat bone marrow mesenchymal stem cells (BM-MSC). RJPBCS 2019;10(2):253–65.
[28] Kentaro A, Yong-Ouk Y, Takayoshi Y, et al. Characterization of bone marrow derived mesenchymal stem cells in suspension. Stem Cell Res Ther 2012;3:40.
[29] Ren J, Huan W, Katherine T, et al. Human bone marrow stromal cell confluence: effects on cell characteristics and methods of assessment. Cytotherapy 2015;17:897–911.
[30] Hammam OA, Elkhafif N, Attia YM, et al. Wharton's jelly-derived mesenchymal stem cells combined with praziquantel as a potential therapy for Schistosoma mansoni-induced liver fibrosis. Sci reports 2016:1–13.
[31] Zeng H, Junhua W, Wenya L, et al. Evaluation of experimentally induced early hepatic alveolar echinococcosis in rats with ultrasonography. Radiol Infec Dis 2016;3:114–9.
[32] Tripathi TMS, Khan HM, Mahendra PSN, et al. Modulation of in vivo immunoglobulin production by endogenous histamine and H1R and H2R agonists and antagonists Pharmacol report62; 2010. p. 917–25.
[33] Qureshi MA, Havenstein GB. A comparison of the immune performance of a 1991 commercial broiler with a 195 random bred strain when fed typical '195 and 1991 broiler diets. Poult Sci 1994;73:1805–12.
[34] Radfar MH, Mehdi BZ, Mehdi B, et al. Hematological, biochemical and pathological findings in goats naturally infection with Cysticercus tenuicollis. J Parasit Dis 2014;38(1):68–72.
[35] Coligan JE, Kruisbeek AM, Margulies DH, et al. ACK lysing buffer. In: John Wiley and Sons, eds. Current Protocols in Immunology. New York, NY: E-Publishing Inc; 1993. p. 3–5.
[36] SPSS Statistical Package for Social Sciences. Chicago, IL, USA Copyright©for Windows: SPSS Inc; 2007. version 160.
[37] Dominici M, Blanc K Le, Mueller I, et al. Minimal criteria for defining multipotent mesenchymal stromal cells. Inter Soci Cell Ther posit stat. Cytother. 2006;8(4):315–7.
[38] Hussein HA, Elrashidy M. Ultrasonographic features of the liver with cystic echinococcosis in sheep. Vet Rec Open 2014;1:e000004.
[39] Kodama Y, Fujita N, Shimizu T, et al. Alveolar Echinococcosis: MR findings in the liver. Radiology 2003;228:172–7.
[40] MiLicevic MN. In: Blumgart LH, Fong Y, editors. Hydatid disease: surgery of liver and biliary tract. 3rd ed. London: W B. Saunders Company Ltd; 2000.
[41] Khuroo MS. Hydatid disease: current status and recent advances. Ann Saudi Med 2002;22:56–64.
[42] Díaz A, Casaravilla C, Barrios AA, Ferreira AM. Parasite molecules and host responses in cystic echinococcosis. Parasite Immunol 2016;38(3):193–205.
[43] Zhang S, Hue S, Hue D, et al. Vuitton. Expression of major histocompatibility complex class I chain-related molecule A, NKG2D, and transforming growth factor-α in the liver of humans with alveolar echinococcosis: new actors in the tolerance to parasites? J Infect Dis 2008b;197:1341–9.
[44] Davies JE, Walker JT, Keating A. Concise review: Wharton's jelly: The rich, but enigmatic, source of mesenchymal stromal cells. Stem Cells Trans Med 2017;6(7):1620–30.
[45] Rawat S, Suchi G, Sujata M. Mesenchymal stem cells modulate the immune system in developing therapeutic interventions. In: Immune Response Activation. Intech Open; 2019 [Chapter].
[46] Wang J, Haozhen R, Xianwen Y, et al. Interleukin-10 secreted by mesenchymal stem cells attenuates acute liver failure through inhibiting pyroptosis. Hepatol Res 2018;48:E194–202.
[47] Sala E, Genua M, Petti L, et al. Mesenchymal stem cells reduce colitis in mice via release of TSG6, independently of their localization to the intestine. Gastroenterol 2015;149:163–76.
[48] Mejri N, Müller J, Gottstein B. Intraperitoneal murine Echinococcus multilocularis infection induces differentiation of TGF-β-expressing DCs that remain immature. Parasite Immunol 2011a;33:471–82.
[49] Mejri N, Müller N, Hemphill A, Gottstein B. Intraperitoneal Echinococcus multilocularis infection in mice modulates peritoneal CD4+ and CD8+ regulatory T cell development. Parasitol Int 2011b;60:45–53.

[50] Budke CM, Casulli A, Kern P, Vuitton DA. Cystic and alveolar echinococcosis: successes and continuing challenges. PLoS Neglected Trop Dis 2017;11(4): e0005477.
[51] Gazdic M, Aleksandar A, Bojana SM, et al. Mesenchymal stem cell-dependent modulation of liver diseases. Int J Biol Sci 2017;13.
[52] Gazdic M, Volarevic V, Arsenijevic N, et al. Mesenchymal stem cells: a friend or foe in immune-mediated diseases. Stem Cell Rev 2015;11:280–7.
[53] Kayagaki N, Wong MT, Stowe IB, et al. Non canonical inflammasome activation by intracellular LPS independent of TLR4. Science 2013;341:1246–9.
[54] Chen W, Huang Y, Han J, et al. Immunomodulatory effects of mesenchymal stromal cells-derived exosome. Immunol Res 2016;64(4):831–40.
[55] Fridman R. Matrix metalloproteinases. Biochimica et Biophysica Acta. Mol Cell Res 2010;1803(1):1–2.
[56] Karen E. Mechanisms of mesenchymal stromal cell immunomodulation. Immunol Cell Biol 2012;91(1):19–26.
[57] Németh K, Leelahavanichkul A, Yuen PS, et al. Bone marrow stromal cells attenuate sepsis via prostaglandin E (2)-dependent reprogramming of host macrophages to increase their interleukin-10 production. Nat Med 2008;15(1):42–9.
[58] Schu S, Nosov M, O'Flynn L, et al. Immunogenicity of allogeneic mesenchymal stem cells. J Cell Mol Med 2012;16(9):2094–103.